Solid State Communications 252 (2017) 59–63

Contents lists available at ScienceDirect

Solid State Communications

journal homepage: www.elsevier.com/locate/ssc

Communication

Structural, vibrational and magnetic properties of the orthoferrites $LaFeO_3$ and $YFeO_3$: A comparative study

P.V. Coutinho, F. Cunha, Petrucio Barrozo*

Departamento de Física, Universidade Federal de Sergipe, Rod. Marechal Rondon, s/n, 49100-000, São Cristóvão, SE, Brazil

ARTICLE INFO

Keywords:
A. Perovskite
B. Combustion method
D. Multiferroic
D. Spin-phonon coupling
D. Magnetic properties

ABSTRACT

We performed this work in order to compare several properties of two orthoferrites: $LaFeO_3$ and $YFeO_3$. Specifically, we have concentrated on the distortions induced in the bulk material due to the exchange between elements with different atomic radii in the individual A sites of perovskite. We investigate the effect of the distortion in the structural, vibrational and magnetic properties. All samples were prepared by combustion method using citric acid as the combustible. The large difference between the ionic radii of the elements on the A site within the perovskite structure Y (r=1.10 Å) and La (r=1.36 Å) induces remarkable changes in the perovskite structure and in its properties. These changes are more noticeable in the reduction of the lattice parameters and in increase of the octahedral distortion. Changes in the Raman modes and in the magnetic properties also are observed. These studies indicate the existence of spin-phonon coupling in the $LaFeO_3$ and $YFeO_3$ structures. The increasing of the distortions on crystalline structure also induces an increase the canting of the spin lattice and consequently an increase of the ferromagnetic component.

1. Introduction

Materials with the perovskite structure present a chemical formula ABX_3, where usually A is a cation with a larger ionic radius, very often a rare earth, an alkaline or alkaline earth metal. B is usually a cation with a smaller radius belonging to the family of the transition metals whereas X is an anionic species, usually Oxygen. The large vantage of this class of material is that almost every atomic species found in the periodic table could be accommodated in the perovskite structure. This remarkable property turns the perovskite an ideal template for obtain new materials with engineered properties, which can be tuned to reach desired applications through substitution or doping.

Usually the complex oxides are produced by solid-state reaction method. However, the presence of the secondary phases commonly found in material produced by this method have stimulated develop new methods with higher efficiency. The major difficulty observed in the production of material by solid state reaction is the bad homogeneity of the powder. This hindrance leads to the necessity of several thermal treatments intercalated with intermediary grindings. Between the new techniques that have been developed to produces materials free of secondary phases we highlight the sol-gel, Pechini and combustion method. The combustion of the method has attracted attention by to be a fast, effective and inexpensive process. Furthermore, this technique has shown hope to achieve nanostructured materials [1].

Orthoferrites usually crystalize in a distorted perovskite structure of the kind $AFeO_3$, with space group *Pnma* (group 62, D_{2h}^{16}). In this structure, Fe ions are coordinated to six oxygen anions, resulting in octahedral with the iron ion is located on its center. The cationic species A stands in the interstitial area between the octahedral structures and is coordinated by 12 Oxygen anions. [2]. A lanthanide orthoferrite presents a pseudo cubic conformation, where $a \approx b \approx \sqrt{2}\,a_{pc}$, and $c \approx 2a_{pc}$. Here a_{pc}, is the cell parameter of a pseudo cubic structure. This kind of distortion is very usual among the perovskites and remains stable when the Goldschmidt factor $t=\frac{r_A+r_0}{\sqrt{2}\,(r_B+r_0)}$, is smaller than 0.975. The Yttrium orthoferrite also presents an orthorhombic cell, however its symmetry is considerably smaller [3]. The Goldschmidt factors for the Lanthanum and Yttrium orthoferrites are respectively 0.954 and 0.855.

The orthoferrites containing diamagnetic ions in the A site usually present an antiferromagnetic ordering, where the Néel temperature lies below 750 K. The presence of a Dzyaloshinskii-Moriya (DM) interaction in some materials containing iron in its structure can leads to a canting of the spin-lattice, resulting a weak ferromagnetic ordering in these materials [4,5]. The magnetic transition temperature in these materials is closely related to the ionic radius of the A site element where the transition temperature increases with the ionic radius [6]. The materials we have studied, $LaFeO_3$ and $YFeO_3$, display a transition

* Corresponding author.
E-mail address: pbs@ufs.br (P. Barrozo).

http://dx.doi.org/10.1016/j.ssc.2017.01.019
Received 26 August 2016; Received in revised form 14 December 2016; Accepted 18 January 2017
Available online 19 January 2017
0038-1098/

from antiferromagnetic to paramagnetic respectively at 740 K and 655 K [7,8]. Recently some groups have shown that it is possible to attain ferroelectricity in the centrosymmetric orthoferrites. Archarya et al. [9] demonstrated in 2010 the existence of measurable hysteresis in $LaFeO_3$. Similar effect was published by Shang et al. [7] in 2012 indicating a ferroelectric ordering in $YFeO_3$. These results suggest the existence of multiferroic properties in both materials. There are however little studies so far about the multiferroic properties and its origin in such materials. The determination of the distortion in crystalline structure of the $LaFeO_3$ and $YFeO_3$ and its effect in the vibrational and magnetic properties is the main purpose of this study.

2. Material and methods

The samples were produced by the combustion method. The method consists of mixing metallic salts with a combustible in an aqueous solution. Upon mixing and heat the solution to form a gel and after start a self-propagating reaction combustion. We prepared the chosen samples, namely, $LaFeO_3$ and $YFeO_3$ by first mixing 10 ml of nitric acid 65% to dilute the precursor oxides, Y_2O_3 or La_2O_3, and $Fe(NO_3)_3{\cdot}9H_2O$. The amount of each species was determined to achieve a stoichiometric proportion for each sample. The final solution was obtained adding 1.5 g of citric acid as fuel and also was adding distilled water to reached 50 ml of solution. After gentle mixing, the solution was heated to 100 °C to discard the water excess and reach a gel. Immediately thereafter the sample was heated to 300 °C reaching the ignition point. The resulting material was carefully grinded and thermally treated at 1100 °C for 24 h. This step of the synthesis was necessary to eliminate remaining organic residues and achievement of the desired phase. The last step consisted of compressing the powder into disks 8 mm in diameter and 1 mm thick followed by another 48 h at 1100 °C.

X-ray diffractometry (XRD) was carried out using a Bruker D8 advanced diffractometer operating at the Bragg-Bretano geometry with Cu-K α radiation. The XRD measurement were carried out in range of 20–80° with step of 0.02° using a 1D Lynxeye sensor with 192 channels with time of acquisition of the 1 s. The X-ray diffraction patterns were indexed using the ICSD databases for $LaFeO_3$ (ICSD-164083) and for $YFeO_3$ (ICSD-80866). The experimental patterns were further analyzed using the Rietveld method using the GSAS software. The background of the X-ray diffraction pattern was fitting using a *shifted Chebyshev* with a 11-degree polynomial. The peaks were adjusted with pseudo-voigt function similar to that developed by Stephens et al. [10] which corresponds to the fourth profile of the GSAS software. The unitary cell parameters and the atomic positions were also further refined using the Rietveld method. The crystalline structure artwork was made possible using the Vesta software.

The vibrational spectra of the samples were acquired using a dispersive Raman spectrometer model SENTERRA from Bruker. The measurements were carried out under the microscope objective 20x and with a Laser He-Ne 633 nm at 10 mW. The acquisition time was 120 s and the Raman measurements were acquired in the range between 60 cm^{-1} and 1500 cm^{-1}. The measurements were performed at different sample temperatures starting at room temperature (300 K) up to 720 K. An FTIR600 oven was used to hold the sample whereas a Linkam TP 94 unit controlled its temperature. Magnetic properties were measured using a SQUID magnetometer MPMS-7T from Quantum Design. These measurements were performed at 5 K with magnetic fields up to 7 T.

3. Results and discussion

Fig. 1 presents the X-ray diffractograms of the $LaFeO_3$ and $YFeO_3$ samples. We were not able to verify the appearance of peaks belonging to secondary phases in these samples. The absence of secondary phases was confirmed through Rietveld refinement which also demonstrated

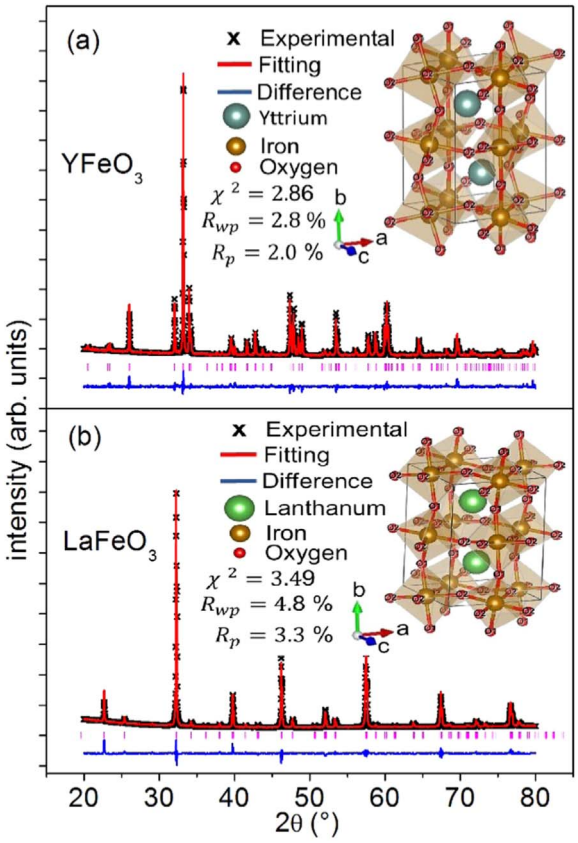

Fig. 1. X-ray diffraction patterns of the $LaFeO_3$ (a) and $YFeO_3$ (b). The black cross are the experimental data, the Rietveld refinement are show by the red lines, and the difference between the experimental data and Rietveld refinements are show by the blue lines. The right inserts show the crystalline structures of the samples obtained using the Rietveld results and the VESTA software, in these crystalline structures A is the site of the Y (a) and La (b), B is the site of the Fe, O1 and O2 are the different sites of the oxygen on the structure. (For interpretation of the references to color in this figure legend, the reader is referred to the web version of this article.)

that both samples present a distorted orthorhombic structure, with the space group *Pnma* (D_{2h}^{16}), in full agreement with the literature [11,12]. The parameters of quality of the refinement are also shown in Fig. 1.

The main peak for $LaFeO_3$ is located at 32.23° and is a convolution of the planes (200), (121) and (002) of the crystal structure. The substitution of the La by Y induces an increase in the octahedral distortion and a reduction of the lattice parameter b and c. Although these changes in the lattice parameter do not induce a structural phase transition, is observed a reduction of the crystal symmetry and it is responsible by the split of the main peaks in the $YFeO_3$ as is observed in Fig. 1. These changes in the lattice parameters can be attributed to difference between the ionic radius of the La and Y. These changes were also observed by Cristóbal et al. [13]. The summarization of the data obtained from the Rietveld refinement is shown in (Table 1)

The diagrams of the crystal structures are also shown as right insert in Fig. 1. It is easily perceivable that $YFeO_3$ presents a larger distortion of the octahedral structures when compared to $LaFeO_3$. This feature can be observed by the reduction of the angles Fe-O1-Fe and Fe-O2-Fe in the $YFeO_3$ compound.

Fig. 2 shows the Raman spectra of the samples $LaFeO_3$ and $YFeO_3$. As expected the active region for the main vibrational modes of the orthoferrites is below 600 cm^{-1} in good agreement with already published results [14–18].

Our results indicate that vibrational modes associate with the elements in "A" site of perovskite are located below 200 cm^{-1} for $LaFeO_3$ and below 240 cm^{-1} for $YFeO_3$. The substitution of La by Y in the orthoferrites induces a decrease of the lattice parameter that is

Table 1
Crystallographic parameter obtained by Rietveld refinement.

Parameters	$LaFeO_3$	σ (LaFeO3)	$YFeO_3$	σ (YFeO3)
Space group	Pnma		Pnma	
a (Å)	5.5621	0.0001	5.5916	0.0001
b (Å)	7.8516	0.0002	7.6032	0.0001
c ()	5.5520	0.0001	5.2809	0.0001
Volume ($Å^3$)	242.4635	0.0087	224.5124	0.0029
(La/Y) x	0.0301	0.0002	0.0687	0.0002
y	0.25	0	0.25	0
z	−0.0115	0.0003	0.9798	0.0004
Uiso	0.0761	0.0005	0.1088	0.0008
Fe x	0	0	0	0
y	0	0	0	0
z	0.5	0	0.5	0
Uiso	0.0798	0.0007	0.1031	0.0011
O1 x	0.5069	0	0.4425	0.0018
y	0.25	0	0.25	0
z	0.0987	0	0.107	0.0018
Uiso	0.8	0	0.16	0.0050
O2 x	0.2456	0	0.6845	0.0016
y	−0.0020	0	−0.0604	0.0012
z	−0.3058	0	0.2881	0.0020
Uiso	0.0478	0	0.1974	0.0043
Fe-O1-Fe (°)	148.72	0	142.23	0
Fe-O2-Fe (°)	168.02	0	144.80	0
χ 2	3.49	0	2.86	0
Rwp	4.81%	0	2.80%	0
Rp	3.34%	0	2.00%	0

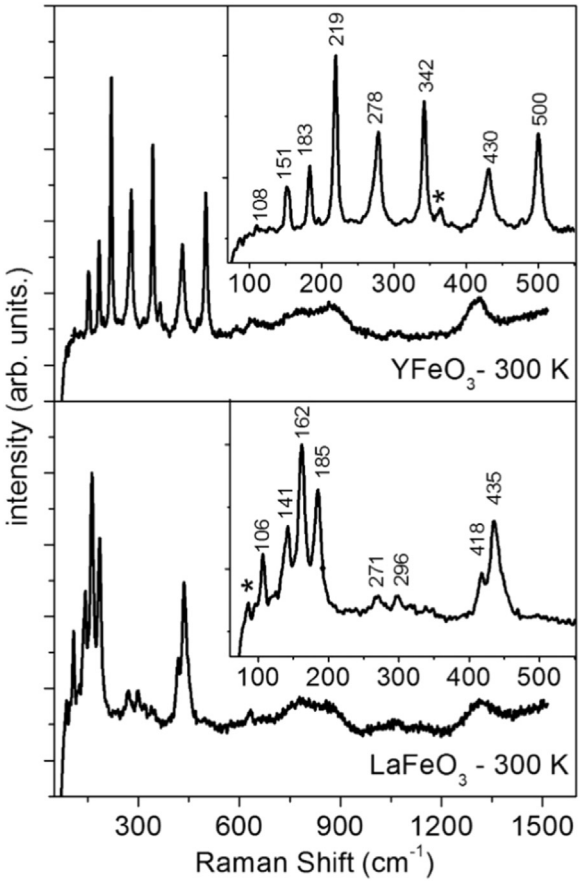

Fig. 2. Normalized Raman spectra of $LaFeO_3$ and $YFeO_3$ at room temperature (300 K). Peaks not found in the literature are highlighted using asterisks.

responsible for a shift of the vibrational modes to the right. This behavior can be attributed to a hardening of the Raman modes due to the increase of the octahedral distortion and by decrease the bond

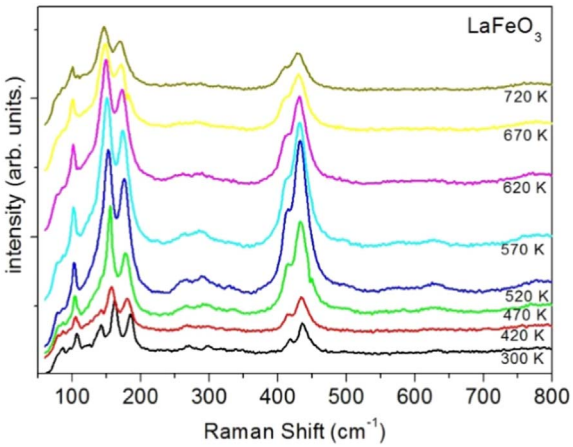

Fig. 3. Raman Spectroscopy for $LaFeO_3$ as a function of the sample temperature.

lengths. These results are in concordance with results of Chanda et al. [19]. The Raman modes associated to the oxygens atoms and the octahedrons are observed between 200 cm^{-1} and 600 cm^{-1} to $LaFeO_3$ and between 240 cm^{-1} and 600 cm^{-1} to $YFeO_3$. Is notable peaks that not have in literature that presenting an asterisk. This peaks, therefore, can be associated with defect of structure, how the absence of A cation or oxygens vacancies. A study about as the change in the stoichiometry of the compound is responsible for the vibrational properties can improve the understand about the spin-phonon coupling in these compounds. We let this as a future perspective to the reader.

In Figs. 3 and 4 are shown the temperature dependence on the Raman spectrum of the samples of $LaFeO_3$ and $YFeO_3$, respectively. It is clearly noticeable that the increase in the temperatures causes a broadening of the peaks in the entire range of measurements. This increase may be attributed to an increase in the short-range disorder, which is a clear signal of the decrease in crystallinity of the material. The increase in temperature also shifts the Raman peaks to lower wavenumber's (data not shown). This change is associated to an increase in the lattice parameter which is explained by a decrease in the elastic constant and the wavenumber. This kind of behavior was already noticed by Mir et al. [20].

It is known that any change in structure and in physical properties of the materials can alter phonons characteristics such as the intensity, frequency and full width at half maximum (FWHM) of the peaks measured by Raman spectroscopy [21]. Although the changes of the peak width and wavenumber with the temperature are still within the expected, it is possible to notice a variation in the peaks intensities. As shown in Figs. 5 and 6 the peaks reach a maximum of intensity between 520 and 570 K. The increase of the peaks Raman intensities

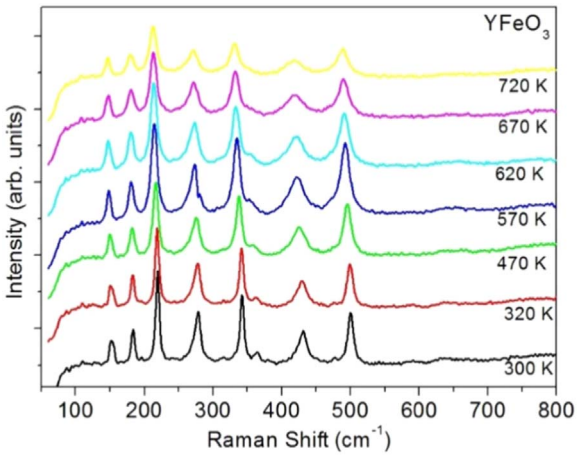

Fig. 4. Raman Spectroscopy for $YFeO_3$ as a function of the sample temperature.

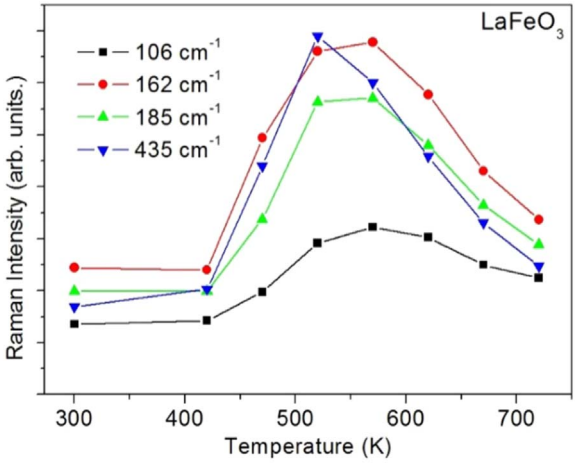

Fig. 5. Raman Peak intensity as a function of temperature of the $LaFeO_3$ sample.

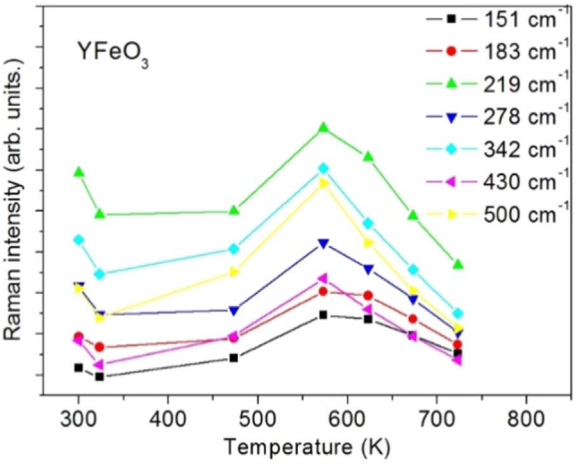

Fig. 6. Raman Peak intensity as a function of temperature of the $YFeO_3$ sample.

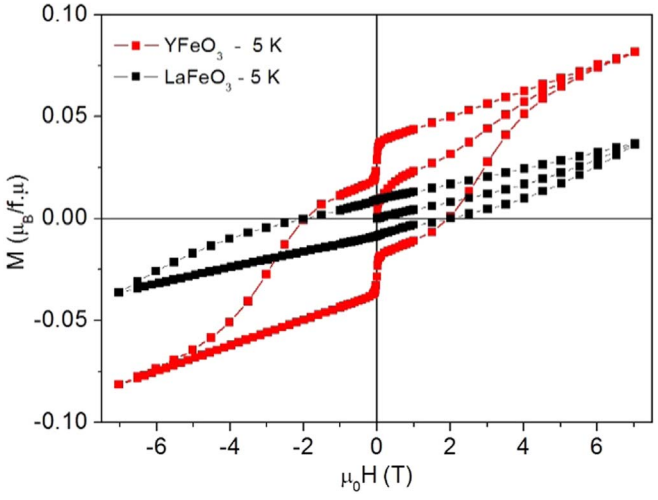

Fig. 7. Magnetic measurements of the samples as a function of the applied magnetic field at 5 K.

close to the magnetic transition temperature can indicate a spin-phonon coupling in these compounds.

A large difference (> 100 K) between the Néel temperature and the temperature where occur the spin-phonon coupling also was observed in BiFeO3 [21]. A possible explained for this is that close Néel temperature we have the formation of ordered cluster and only at far below of Néel temperature we can observe a long-range order and is in this region where we can observe the spin-phonon coupling. The formation of ferromagnetic cluster also was observed in perovskite compounds produced by combustion methods [22].

In Fig. 7 we show the magnetic behavior of both samples as a function of the applied magnetic field at 5 K. The magnetic ordering of these materials is due solely to the Fe^{3+} ion since both Lanthanum and Yttrium do not present a measurable magnetic response. Although both samples have an antiferromagnetic ordering attributed to the super-exchange interaction between the Fe ions. The presence of a Dzyaloshinskii-Moriya (DM) interaction in these materials induces a canting of the spin-lattice which leads to a weak ferromagnetic response. These results are in good agreement with those reported by Mathur et al. [23], Lima et al. [24] and Popa et al. [16].

4. Conclusions

The results shown indicate that the combustion method can be successfully used to produce $LaFeO_3$ and $YFeO_3$ without spurious phases. The X-ray diffractograms with Rietveld refinement indicated that these samples are single phase with orthorhombic distorted structure belonging to the space group *Pnma*. The substitution of Lanthanum by Yttrium leads to a reduction of the lattice parameters, of the Fe-O1-Fe and Fe-O2-Fe angles and a shift to larger wavenumbers of the Raman peaks. On the other hand, the increase of the temperature on the sample, which is responsible for an increase in the lattice parameters, leads to a shift of the Raman modes to low wavenumbers, probably due to a decrease in the chemical bonds strength. The increase of the peaks intensity of the Raman close to magnetic transition temperature indicates the existence of spin-phonon coupling in these compounds. The increase of the octahedral distortion induces an increase of the ferromagnetic. These distortions are closely related with the DM interaction and can be used to improve the magnetic response and also the magnetoelectric coupling in the multiferroic compounds.

Acknowledgements

This work was supported by the Brazilian science agencies CNPq (grant 443458/2014-6). We acknowledge the support of Brazilian Petroleum Agency (ANP) and Petrobras.

References

[1] E. Chinarro, J.R. Jurado, M. Colomer, J. Eur. Ceram. Soc. 27 (2007) 3619–3623.
[2] M.A. Ahmed, M.S. Selim, Mater. Chem. Phys. 129 (2011) 705–712.
[3] C.A. Dixon, C.M. Kavanagh, K.S. Knight, W. Kockelmann, F.D. Morrison, P. Lightfoot, J. Solid State Chem. 230 (2015) 337–342.
[4] R. Saha, A. Sundaresan, C.N.R. Rao, Mater. Horiz. 1 (2014) 20–31.
[5] T. Chakraborty, R. Yadav, S. Elizabeth, H.L. Bha, Phys. Chem. Chem. Phys. 18 (2016) 5316–5323.
[6] M. Eibschutz, S. Shtrikman, D. treves, Phys. Rev. 156 (2) (1967) 562–577.
[7] M. Shang, C.T. Zhang, L. Yuan, L. Ge, H. Yuan, H. Feng, Appl. Phys. Lett. 102 (2013) 062903.
[8] J.W. Seo, E.E. Fullerton, F. Nolting, A. Scholl, J. Fompeyrine, J.P. Locquet, J. Phys.: Condens. Matter 20 (2008) 264014.
[9] S. Acharya, J. Mondal, S. Ghosh, S.K. Roy, P.K. Chakrabarti, Mater. Lett. 64 (2010) 415–418.
[10] W.P. Stephens, J. Appl. Crystallogr. 32 (1999) 281–289.
[11] S.M. Selbach, J.R. Tolchard, A. Fossdal, J. Solid State Chem. 196 (2012) 249–254.
[12] P. Coppens, M. Eibschutz, Acta Crystallogr. 19 (1965) 524–531.
[13] A.A. Cristóbal, P.M. Botta, E.F. Aglietti, M.S. Conconi, P.G. Bercoff, J.M. Porto López, Mater. Chem. Phys. 130 (2011) 1275–1279.
[14] H.C. Gupta, M.K. Singh, L.M. Tiwari, J. Raman Spectrosc. 33 (2002) 67–70.
[15] M. Romero, R.W. Gómeza, V. Marquina, J.L. Pérez-Mazariegoa, R. Escamilla, Physica B: Condens. Matter 443 (2014) 90–94.
[16] M. Popa, J.M.C. Moreno, J. Alloy. Compd. 509 (2011) 4108–4116.
[17] A.P.B. Selvadurai, P. Pazhanivelu, C. Jagadeeshwaran, R. Murugaraj, J. Alloy. Compd. 646 (2015) 924–931.
[18] A.P. kuzmenko, M.B. Dobromyslov, J. Magn. Magn. Mater. 324 (2012) 1262–1264.
[19] S. Chanda, S. Saha, A. Dutta, B. Irfan, R. Chatterjee, T.P. Sinha, J. Alloy. Compd. 649 (2015) 1260–1266.

[20] F.A. Mir, M. Ikrama, R. Kumar, J. Raman Spectrosc. 42 (2011) 201–208.
[21] R. Haumont, J. Kreisel, P. Bouvier, F. Hippert, Phys. Rev. B 73 (2006) 132101.
[22] P. Barrozo, N.O. Moreno, J.A. Aguiar, Adv. Mater. Res. 925 (2014) 122–127.
[23] S. Mathur, M. Veith, R. Rapalaviciute, H. Shen, G.F. Goya, W.L.M. Filho, T.S. Berquo, Chem. Mater. 16 (2004) 1906–1913.
[24] E. Lima Jr, T.B. Martins, H.R. Rechenberg, G.F. Goya, C. Cavelius, R. Rapalaviciute, S. Hao, S. Mathur, J. Magn. Magn. Mater. 320 (2008) 622–629.